Hydrodynamic and mass transfer efficiency of ceramic foam packing applied to distillation

Julien Lévêque, David Rouzineau*, Michel Prévost, Michel Meyer

Université de Toulouse, Laboratoire de Génie Chimique, CNRS/INP/UPS, 5 rue P. Talabot, BP 1301, 31106 Toulouse Cedex 1, France

A B S T R A C T

In addition to a high void volume and specific area, solid foams possess other properties (low density, good thermal, mechanical, electrical, and acoustical behaviour) that make them attractive for applications such as heat exchangers and reformers. Applications using foams as catalysts or structured catalyst supports have demonstrated higher performance than classical catalysts. Several studies have explored the hydrodynamic behaviour of foams in monophasic and countercurrent systems and have reported very low pressure drops. This paper describes the application of ceramic foam to distillation. The β-SiC foam contains 5 pores per inch (PPI) with a 91% void volume and a surface area of 640 m^2/m^3. Performance parameters including pressure drop for the dry and wet packing, flooding behaviour, and dynamic liquid hold-up were measured in a column of 150 mm internal diameter. The mass transfer efficiency in terms of the height equivalent to theoretical plate (HETP) was determined by total reflux experiments using a mixture of *n*-heptane and cyclohexane at atmospheric pressure. The experimental results were used to develop a set of correlations describing pressure drop and liquid hold-up in terms of a dimensionless number. The hydrodynamic performance and mass transfer efficiency were compared with classical packing materials used in distillation.

1. Introduction

Solid foams (either ceramic or metal-based) have been known for many years and have a wide range of applications due to their low density and attractive thermal, mechanical, electrical, and acoustical properties. In the last decade, there has been growing interest in these foams for applications such as heat exchangers, reformers, mixing improvement, and as catalysts or structured catalyst supports (Pestryakov et al., 1996, 2007; Richardson et al., 2000, 2003; Sirijaruphan et al., 2005; Winé et al., 2006; Chin et al., 2006). Foams or other high-porosity cellular materials represent a very promising new class of structural materials. Hydrodynamic measurements reported in the literature (Richardson et al., 2000; Lacroix et al., 2007; Despois and Mortensen, 2005; Bhattacharya et al., 2002; Giani et al., 2005; Dukhan, 2006; Leong and Jin, 2006; Topin et al., 2006; Incerra Garrido et al., 2008) have typically been obtained in monophasic or occasionally biphasic (air/water) systems in cocurrent operation. These studies defined the permeability of the foams and confirmed that foam hydrodynamics follows the Forchheimer relationship (Lacroix et al., 2007):

$$\frac{dP}{dZ} = \frac{\mu}{K}u + \beta\rho u^2 \quad (1)$$

A noteworthy finding of these studies was a low pressure drop in both monophasic and cocurrent biphasic systems. Stemmet et al. (2005) initiated the study of countercurrent hydrodynamics in foams. They also observed a low pressure drop (on the order of a few mbar m^{-1} for liquids with mass velocities in the range of 0–17 kg m^{-2} s^{-1} and gas flux in the range of 0–1 kg m^{-2} s^{-1}) with a biphasic system in countercurrent operation. The flooding behaviour was similar to the Sulzer KATAPAK structured packing (Ellenberger and Krishna, 1999). In a later paper, (Stemmet et al., 2007) studied cocurrent gas–liquid mass transfer in terms of an overall volumetric gas–liquid mass transfer coefficient ($k_L a_{GL}$). This coefficient was found to be relatively high, ranging up to 1.3 s^{-1}. However, the column used in this study was rectangular with a cross section of 30 cm×1 cm. This does not correspond to a realistic situation in distillation and led to significant side effects.

These promising results were the starting point of our study of the application of ceramic foam as a distillation packing material. Several important parameters are required to characterize a new distillation packing material. This paper describes the experimental

* Corresponding author. Tel.: +33 0 5 34 61 52 53; fax: +33 0 5 34 61 52 52.
E-mail address: david.rouzineau@ensiacet.fr (D. Rouzineau).

steps necessary to validate the use of new packing materials, including measurement of the hydrodynamic characteristics to estimate the operating range, pressure drop, and flooding point; and determination of the mass transfer efficiency.

2. Foam structure

Ceramic foams in the form of silicon carbide (β-SiC) studied in this work, exhibit advantageous properties such as high mechanical strength, high heat conductivity, and high resistance to corrosive media. β-SiC foams have medium surface area (15–20 $m^2\,g^{-1}$) and a void volume between 88% and 92%. The foam preparation method developed by the Sicat company, (Patent US 5,429,780; US 5,449,654; EP 0 624 560; EP 0 880 406 B1; US 5,958,831; US 6,251,819; FR2860992, FR2860993, US20050159292, FR2834655) is based on the impregnation of a polyurethane foam with a homogeneous mixture of silicon, charcoal, phenolic resin, and oxygen supplier. After polymerization of the resin, the material is calcined at 1300 °C in an inert atmosphere. The final β-SiC foam product is a reticulated cellular material that replicates the morphology of the polyurethane foam. This method permits the synthesis of β-SiC foams with controlled cell sizes close to the pores per inch (PPI) of the starting polyurethane material. The structural parameters amenable to modification include the pore size (characterized by PPI number), the void volume, and the apparent density. This allows the manufacture of materials with a wide variety of hydrodynamic properties. For this type of foam, the open void fraction is not dependent on the PPI number; in fact it is possible to maintain a constant open void fraction over the entire range of PPI numbers. Conversely, for the same pore diameter, it is possible to have different open void fractions. This may be visualized using the cubic representation of the cells (Fig. 1) described by Giani et al. (2005). The size of the struts (solid phase between the cells) can be changed to obtain a different void volume without changing the PPI number.

Our study is focused on open celled SiC foam with a single PPI number and porosity with the intrinsic characteristics summarized in Fig. 2. The specific area was calculated from the cell diameter and void volume using the following equations (Lacroix et al., 2007), in which $a = \phi/2.3$ and ϕ is the cell diameter; a represent the window diameter. The difference between cell diameter and window diameter is illustrated in Fig. 3. The value obtained for specific area is of 640 m^2/m^3:

$$ds = \frac{a[(4/3\pi)(1-\varepsilon)]^{1/2}}{1-[(4/3\pi)(1-\varepsilon)]^{1/2}} \tag{2}$$

$$a_c = \frac{4}{ds}(1-\varepsilon) \tag{3}$$

3. Experimental set up and methods

3.1. Hydrodynamics pilot plant

The experimental setup for hydraulic studies is illustrated in Fig. 4. Foam cylinders were placed in a glass column with an internal diameter of 150 mm and a packing height of up to 90 cm. The column was operated in a countercurrent mode with an air–water system. The studies were carried out at room temperature under atmospheric pressure.

The liquid flowed from a tank through a pump and flowmeter and was supplied to the top of the column via a plate distributor containing 2716 holes per square metre for liquid flow to assure good

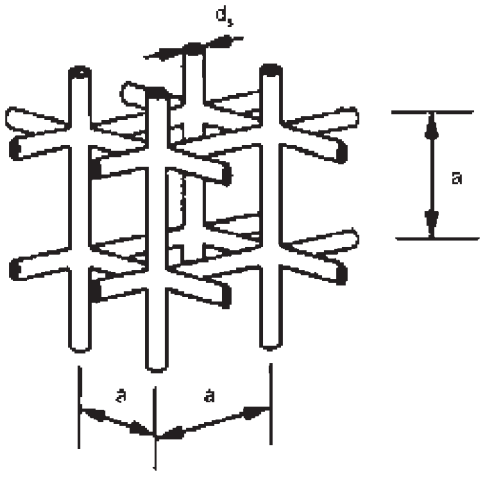

Fig. 1. Representation of cubic model of Giani et al. (2005).

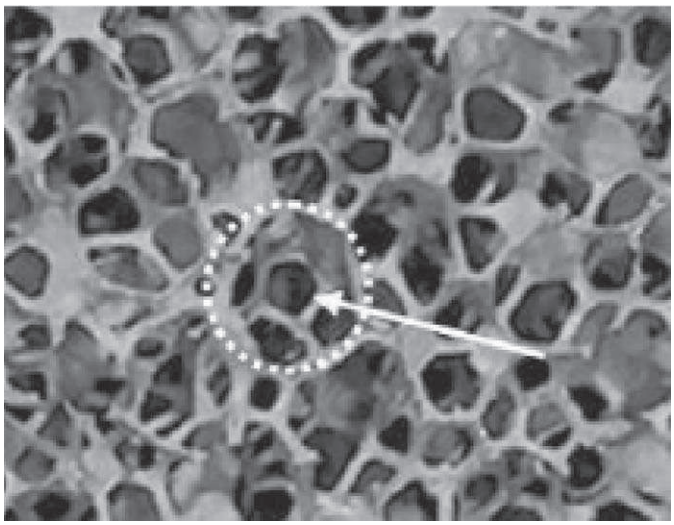

Fig. 3. Optical picture of SiC foam. Dotted circle show the cell diameter whereas white arrow indicate a pentagonal window.

Company: Sicat
Materials: β Silicium Carbide
Average cell diameter: 5 350 µ (5 PPI)
Cylinder diameter : 139 à 146 mm
Height : 92-99 mm
Apparent density: 130-140 g/l
Void volume: 92%
Specific area: 640 m^2/m^3

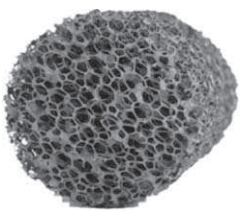

Fig. 2. Characteristics of β-SiC foam studied.

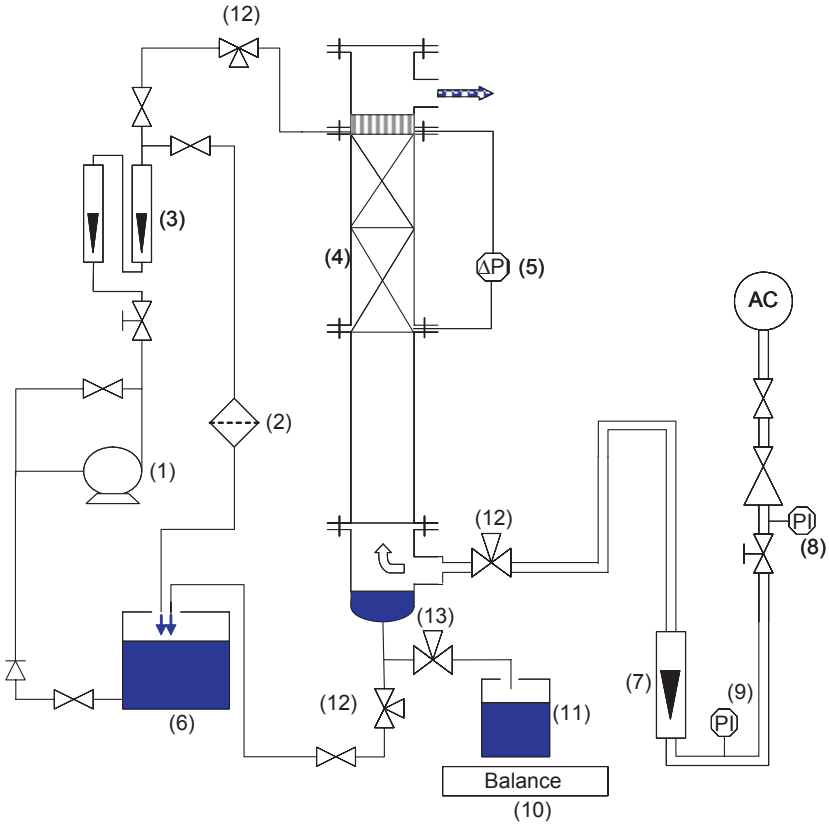

Fig. 4. Experimental setup for hydraulic experiments: (1) centrifugal pump; (2) filter; (3) liquid flowmeter; (4) packed column; (5) U-tube filled with water; (6) tank; (7) gas flowmeter; (8), (9) manometers; (10) balance; (11) tank; (12) electrovalve; and (13) drainage valve.

liquid distribution and a bypass section of 33% for gas flow. The liquid was collected in the tank after passing through the packing. During operation, the liquid superficial velocities were varied between 1 and 10 $m^3\,m^{-2}\,h^{-1}$. The gas flow was supplied at the bottom of the column and was measured using a series of two flowmeters to obtain gas superficial velocities from 0 to 2 $m\,s^{-1}$ in the empty column. The pressure drop was measured using a U-tube manometer filled with water which was inclined to provide a more sensitive measurement (sensitivity of 0.05 mbar).

3.2. Method for hydrodynamic study

The pressure drop was measured by periodically increasing the gas flow at a constant liquid flow until flooding occurred. The flooding point was defined as the point where a reversal of liquid flow appears, the liquid is unable to flow through the packing, the pressure drop along the bed fluctuated, and measurement was impossible due to the instability of the system.

Measurements of liquid hold-up were also carried out using the same apparatus. Liquid hold-up, which represents the amount of liquid retained in the packing, is the sum of two components, the static liquid hold-up (h_Ls) and the dynamic liquid hold-up (h_Ld):

$$h_Lt = h_Ls + h_Ld \tag{4}$$

Dynamic liquid hold-up was measured using the volumetric or drainage method (Buchanan, 1969; Dmitrieva et al., 2005; Muzen and Cassanello, 2005). After steady-state conditions were established, the supply of liquid and gas was stopped by closing three electrovalves (12, Fig. 4). The draining liquid was collected for 30 min and measured using a balance. The dynamic hold-up was calculated by dividing the volume of liquid by the packing volume. Before each test, a high liquid flow was passed through the packing for 30 min to fully wet the foam and eliminate dry zones. Static liquid hold-up could be measured by a similar method than dynamic liquid hold-up. A foam piece was submersed in the liquid, removed and suspended allowing the drainage of liquid. The difference between the initial weight and the weight after drainage constitute the static liquid hold-up. Static liquid hold-up may also be determined from dynamic liquid hold-up results by plotting dynamic liquid hold-up as a function of liquid superficial velocity.

3.3. Distillation pilot plant

The mass transfer efficiency was reported in terms of the height equivalent of theoretical plate (HETP) number obtained by dividing the height of the packing by the number of equilibrium stages (NET).

The HETP experiments were performed using the distillation pilot plant described in Fig. 5. The mixture in the reboiler was heated with steam provided by a 60 kW electrical generator at 8 bar maximum pressure. The heat duty was calculated by measuring the condensate flow of water at the reboiler exit. The temperature of the reboiler and the head of the column was measured with a thermocouple. The standard experimental methodologies developed by Fractionation Research Inc. (FRI) and the Separation Research Program (SRP) were employed to determine the HETP of the packing material. Measurements were carried out by separating a binary mixture by distillation at total reflux. The procedure consisted of

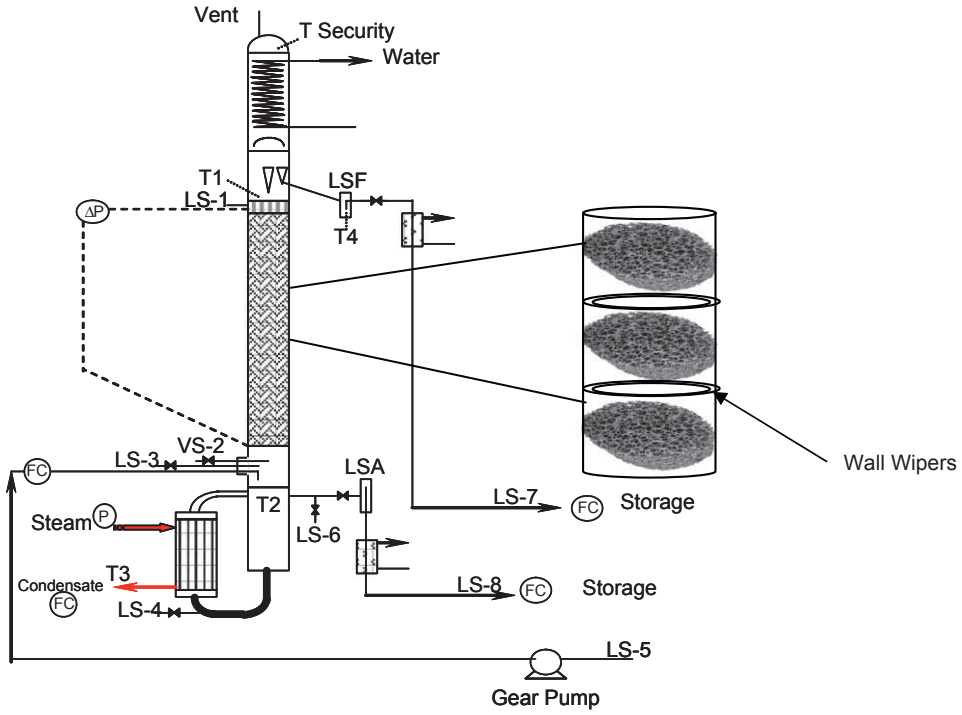

Fig. 5. Experimental setup for HETP tests: (FC) flow control; LS-i, VS-i: liquid Sample n°i, vapour Sample n°i; (ΔP) pressure drop measurement; Tk: temperature measurement n°k; LSA, LSF: liquid seal adjustable, fixed; and (P) pressure indicator.

reaching the flood point, backing off to roughly 20% of flood to unload the bed, and then performing the test at the targeted reboiler duty. The experiments were carried out at atmospheric pressure with a standard cyclohexane/*n*-heptane mixture (Subawalla et al., 1997; Olujic et al., 2000). The required range of reboiler duty was estimated from the corresponding hydrodynamics results and the tests were performed at duties ranging from 2 to 8 kW. The heat losses of the pilot plant were estimated beforehand at approximately 1.25 ± 0.11 kW. Heat losses were determined by operating under no reflux condition, the measurement of distillate flow allowing to determine condenser heat duty. Difference between reboiler and condenser heat duty represent the heat losses.

The first tests were carried with a common packing material (Raschig rings 15×15 mm) to benchmark our method and results. A final test using a different starting composition in the reboiler was performed to determine whether the performance was influenced by the starting composition.

Liquid samples were removed from the top and bottom of the column and analysed using a refractometer. The time between the initial generation of vapour and collection of the first samples was almost 3 h, and the system was considered to be at steady state when three successive samples had the same composition. The top and bottom compositions were used to calculate the NET.

For all of the experiments, wall wipers were inserted between each cylinder of foam to avoid wall effects (liquid flowing on the wall of the column and bypassing the packing).

The pressure drop, liquid hold-up and HETP are reported as a function of the *F*-factor, defined as the product of the superficial vapour velocity and the square root of vapour density:

$$F = u_G\sqrt{\rho_G} \tag{5}$$

4. Experimental results

4.1. Pressure drop and hold-up results

The pressure drop per metre for the dry and wet packing material at different liquid loadings is plotted in Fig. 6(a). The hydrodynamic behaviour was similar for all liquid flowrates; the slopes of the curves are nearly the same and display an increase in pressure drop with increasing liquid and gas velocities. At higher pressure drops, a discontinuity divides the curve into two distinct zones. The location of the discontinuity corresponds to the loading point (this is depicted in Fig. 6(b) for two liquid velocities). The last point of each curve corresponds to the highest recorded pressure drop and represents the flooding point.

Since the terms of the Forchheimer Eq. (1) are difficult to relate to structural characteristics, the models used to determine the permeability of foams are derived from correlations developed for granular beds. Several researchers have used Ergun's model to predict dry pressure drop by modifying the Ergun parameters to fit their experimental data:

$$\frac{\Delta P}{Z} = E_1\frac{\mu(1-\varepsilon)^2}{\varepsilon^3 d_P^2}u_G + E_2\frac{\rho(1-\varepsilon)}{\varepsilon^3 d_P}u_G^2 \tag{6}$$

where u_G is the gas velocity ($m\,s^{-1}$), ΔP the pressure drop (Pa), Z the height of the foam (m), μ and ρ are the fluid viscosity and fluid density, E_1 and E_2 are Ergun constants, ε the bed porosity, and d_P the mean particle diameter of the granular medium. The approach proposed by Lacroix et al. (2007) may be used to calculate d_P:

$$d_P = \tfrac{6}{4}d_S \tag{7}$$

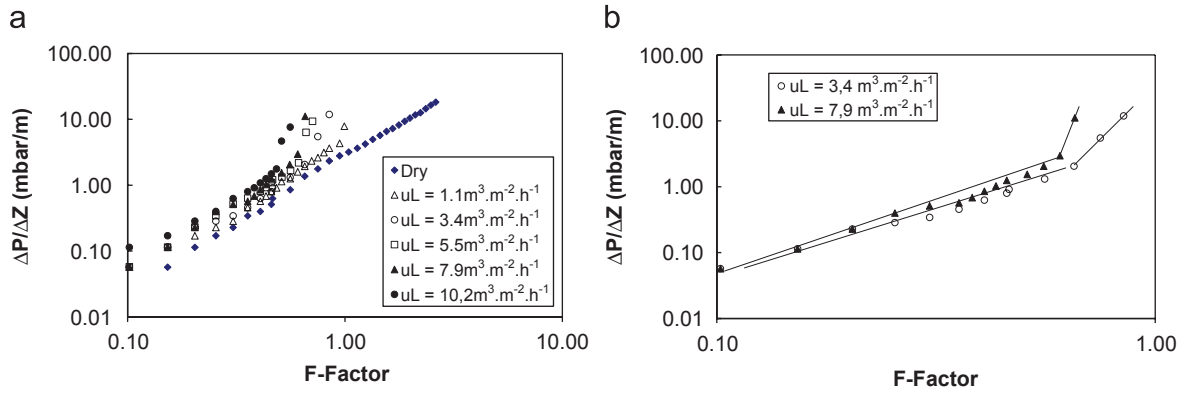

Fig. 6. (a) Pressure drop measurements for dry and wet packing for different liquid velocities and (b) detail of loading zone for two liquid velocities.

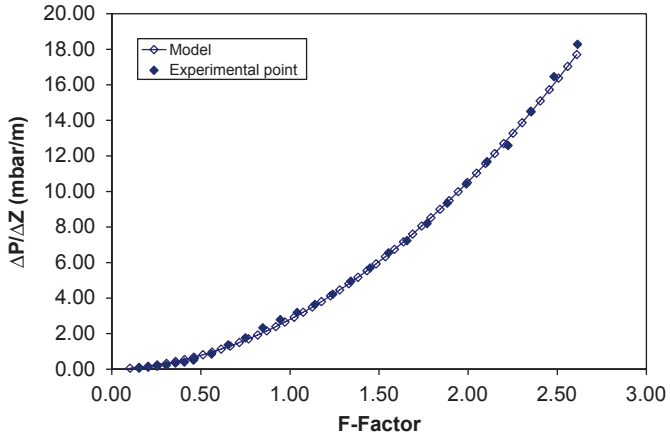

Fig. 7. Comparison of dry pressure drop estimated with experimental data.

Ergun proposed a value of 150 for E_1 and 1.75 for E_2 in the case of columns containing spherical packing materials, but a better fit to our experimental data was obtained with the values $E_1 = 150$ and $E_2 = 1.9$. A comparison of the model and experimental values is presented in Fig. 7 and model shows a good agreement with experimental values.

However, Incerra Garrido et al. (2008) have put in evidence that the modified Ergun equation proposed by Lacroix et al. (2007) is not so convenient for pressure drop prediction and not applicable for all type of foam. In fact, their work shows a considerable deviation (almost 20%) between pressure drop of foam sample with similar structure (PPI number and voidage); this deviation is due to the imperfections of the foam like closed pore. The imperfections of the foam and the quality of foam differ considerably for each manufacturer resulting in such deviation of literature results. That is why one of their important conclusions is that no general model for prediction of pressure drop can be achieved currently. Incerra Garrido et al. (2008) proposed a new empirical model which seems to be more convenient. It is based on the Forchheimer equation with empirical determination of the permeability and inertial coefficient defined with the following equations:

$$\frac{\Delta P}{\Delta Z} = \frac{\mu}{k_1} u_0 + \frac{\rho}{k_2} u_0^2 \tag{8}$$

$$k_1 = 1.42 \times 10^{-4} \left(\frac{D_p}{m}\right)^{1.18} \varepsilon_h^{7.00} \tag{9}$$

$$k_2 = 0.89 \left(\frac{D_p}{m}\right)^{0.77} \varepsilon_h^{4.42} \tag{10}$$

with m defined in the dimensionless number Fg,

$$Fg = \left(\frac{D_p[m]}{0.001m}\right)^m (\varepsilon_h)^n \tag{11}$$

The application of this model require the determination of some supplementary measurements like the determination of ε_h by mercury porosimetry and mass transfer measurements to attain the value of the parameter m.

However, the Lacroix model is used in this work rather than Incerra Garrido et al. model for several reasons.

The foam used in this work is from the same manufacturer than Lacroix et al. (2007), that is why their approach was used for prediction of dry pressure drop. Moreover, the deviations between literature data are more pronounced for high superficial velocities (higher than $5\,m\,s^{-1}$); the upper value of our range of velocity is $2\,m\,s^{-1}$ so the application of Lacroix model is possible in this case. Nevertheless, the authors are aware that the application of this model is limited to our foam.

The similarity of the slopes suggests that the wet pressure drop is dependent on the dry pressure drop and an additional term to characterize the liquid flowing through the packing. Plotting the pressure drop for the wet packing as a function of the dry pressure drop yields a straight line with a higher slope for greater liquid superficial velocities. The pressure drop of wet packing materials below the loading point may be described by an expression of the following form Kolodziej et al. (2004):

$$\frac{\Delta P}{Z} = A\, Re_L^B \left(\frac{\Delta P}{Z}\right)_{Dry} \tag{12}$$

Values of 1.1 and 0.2 were obtained for the empirical coefficients A and B. The values predicted by this model are compared with the experimental data in Fig. 8. In general, the predicted values are quite lower than experimental results with the maximum deviation for low liquid velocity; but the model seems to be in agreement with experimental values. Like for dry pressure drop, the deviation between model and experimental points may be explained by the imperfections of foam which are not taken into account in the correlation.

The pressure drop characteristics of the dry packing are compared to an aluminium foam of similar morphology (5 PPI with 92% void volume) in Fig. 9 (Stemmet et al., 2005). The pressure drops of the aluminium and SiC foam are in the same range of values (several $mbar\,m^{-1}$) even if a slight difference exists for low gas flow. This difference is due to the structure of SiC foam which is not perfect

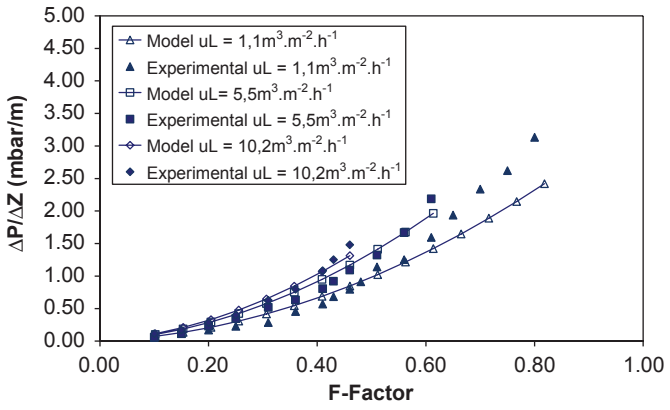

Fig. 8. Comparison of wet pressure estimated and experimental data for three different superficial liquid velocities.

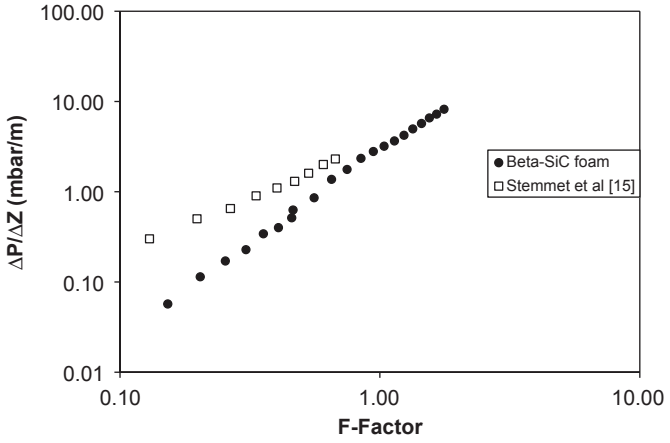

Fig. 9. Pressure drop of dry packing materials for different foams.

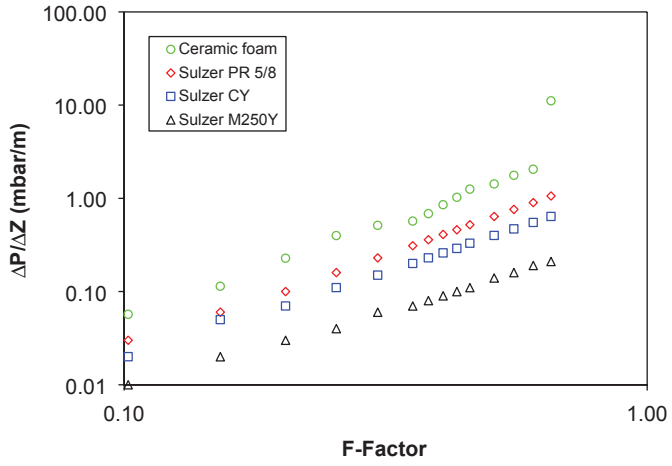

Fig. 10. Pressure drop of ceramic foam, M250Y, CY, and PR 5/8 for $u_L = 7.9\,m^3\,m^{-2}\,h^{-1}$.

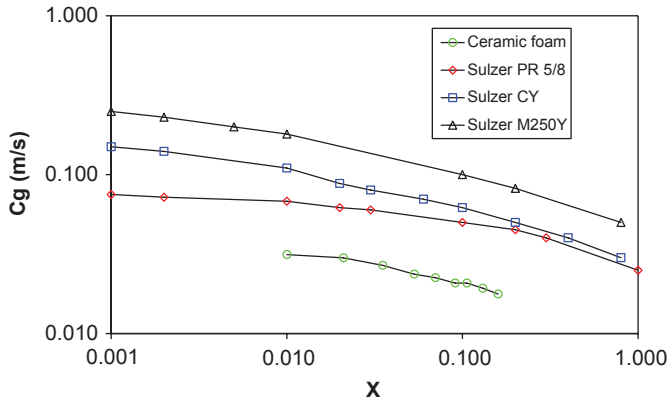

Fig. 11. Flooding line for ceramic foam, M250Y, CY, and PR 5/8.

(some pores are closed on the wall of cylinders), which confirms the observations of Incerra Garrido et al. (2008).

The pressure drop was also compared with three classical packing materials used for distillation, two structured and one random. These were Sulzer M250Y, widely used in industry, with a specific area of $250\,m^2/m^3$; Sulzer CY with a specific area of $700\,m^2/m^3$; and Sulzer 5/8 in Pall rings (denoted as PR 5/8), the dimensions of which are representative of packing materials commonly used in 150 mm diameter columns, with a specific area of $360\,m^2/m^3$.

The hydrodynamic characteristics of these packing materials as a function of the operating conditions may be obtained using the Sulcol software of Sulzer. As an example, the pressure drop for one liquid loading is depicted in Fig. 10 for $u_L = 7.9\,m^3\,m^{-2}\,h^{-1}$. The pressure drop of the foam is somewhat higher than the three other packing materials but within the range of acceptable performance and of the same order of magnitude (several mbar m^{-1}). These findings are logical since M250Y and the Pall rings have a lower specific area. The CY packing has a lower pressure drop than ceramic foam despite having a higher specific area; this is probably due to the higher void volume of CY.

Another very important design parameter for packed columns is the flooding line, because it determines the range of useful flows during distillation. The flooding line may be described in terms of the flowing factor at flooding and the loading factor at flooding calculated using the following relations:

$$X = (L/Gf).\sqrt{(\rho_G/\rho_L)} \tag{13}$$

$$Cg = \frac{Gf}{\sqrt{\rho_G(\rho_L - \rho_G)}} \tag{14}$$

Fig. 11 contains a comparison of the flooding lines for the different packing materials. The flooding line of the foam is lower than the other materials, indicating that flooding occurs at lower liquid and gas flowrates and somewhat restricting the distillation operating range.

In Fig. 12(a), the dynamic liquid hold-up results are plotted for four liquid superficial velocities from 3.4 to 9.1 $m^3\,m^{-2}\,h^{-1}$. The overall shape of the curves corresponds well to theoretical hold-up curves for packing materials; i.e. the liquid hold-up is independent of the gas superficial velocity in the first part of the curve, while in the second part of the curve (the loading zone) the liquid hold-up increases with gas superficial velocity. Liquid hold-up is also influenced by the liquid superficial velocity, increasing as the velocity increases. This can be explained by the fact that at low gas velocities the hold-up consists only of the liquid film at the surface of the packing. The increase in hold-up observed in the loading zone results from the appearance of waves at the liquid film surface that increase the volume retained in the column. The Sulcol software only provides the total liquid hold-up, and in order to make comparisons to other packing

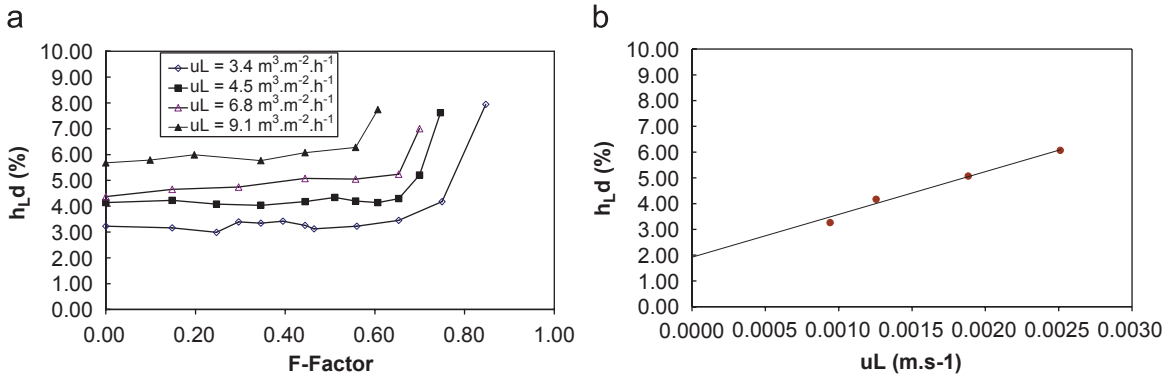

Fig. 12. (a) Dynamic liquid hold-up of ceramic foam as a function of gas velocity and (b) a function of liquid velocity for $u_G = 0.392\,\mathrm{m\,s^{-1}}$.

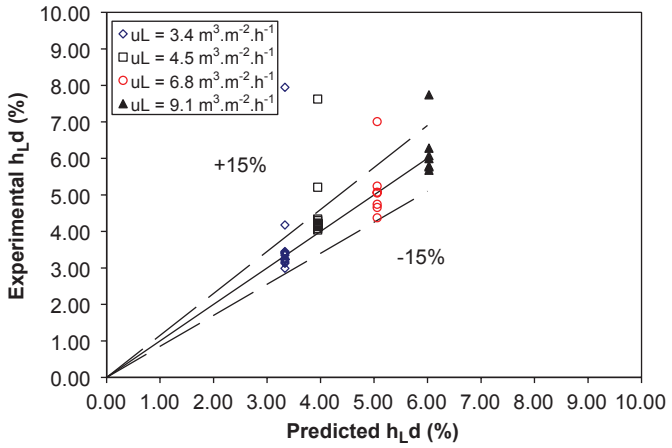

Fig. 13. Comparison between predicted dynamic liquid hold-up and experimental dynamic liquid hold-up.

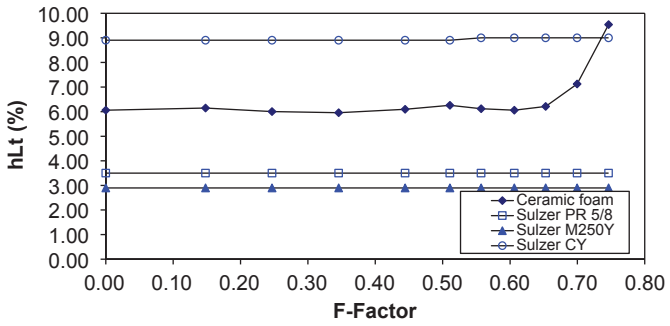

Fig. 14. Liquid hold-up of ceramic foam, M250Y, CY, and PR 5/8 for $u_L = 4.5\,\mathrm{m^3\,m^{-2}\,h^{-1}}$.

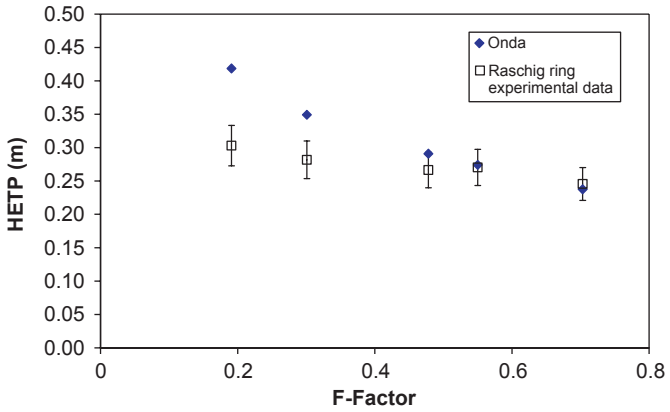

Fig. 15. Comparison of experimental values with Onda correlation values for Raschig rings.

materials it is necessary to determine the static hold-up. One method of estimating the static liquid hold-up consists of plotting the dynamic liquid hold-up as a function of liquid superficial velocity. The y-intercept of the line corresponds to the static liquid hold-up of the packing. This is demonstrated in Fig. 12(b) for a gas superficial velocity of $0.392\,\mathrm{m\,s^{-1}}$. Averaging the values obtained at various gas velocities yields an estimate of 1.9% for the static hold-up.

The dynamic liquid hold-up may be expressed as a power function of the liquid-phase Reynolds number:

$$h_L d = 0.0115\, Re_L^{0.6} \tag{15}$$

A comparison of the model and experimental results is presented in Fig. 13. The deviation of the experimental points from the model prediction does not exceed 15% except for values in the loading zone.

In the comparison with other packing material depicted in Fig. 14, the liquid hold-up of the foam is higher than the hold-up of M250Y and the Pall rings in the region before the loading zone. The rapid increase in liquid hold-up occurs at lower liquid and gas velocities. Like pressure drop, the liquid hold-up of a packing material depends on the specific area, with foams typically displaying higher liquid hold-up values. The liquid hold-up of CY is higher than the foam probably because of the structure (high specific area) and construction material (gauze packing). Increased liquid hold-up at low F-factors will result in high residence times.

4.2. Mass transfer results

4.2.1. Method validation

The results of tests performed using glass Raschig rings with nominal dimensions of 15×15 mm are provided in Fig. 15. The experimental method and results were validated by using the correlation of Onda et al. (1968) to determine the liquid and gas mass transfer coefficients k_L and k_G and to calculate HETP:

$$k_L\left(\frac{\rho_L}{g\mu_L}\right)^{1/3} = 0.0051\left(Re_L\frac{a_c}{aw}\right)^{2/3} Sc_L{}^{-0.5}(a_c d)^{0.4} \tag{16}$$

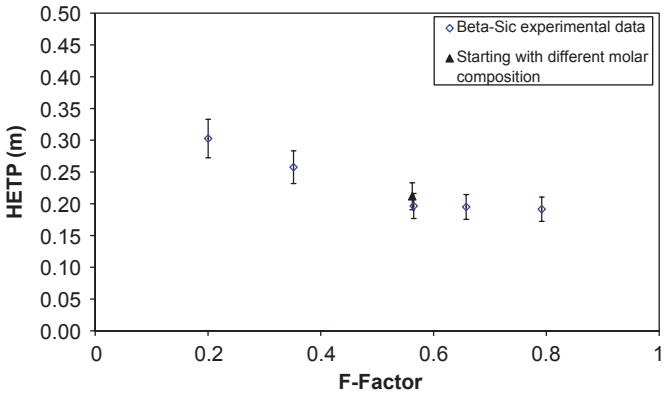

Fig. 16. HETP measurement with ceramic foam for different reboiler heat duty.

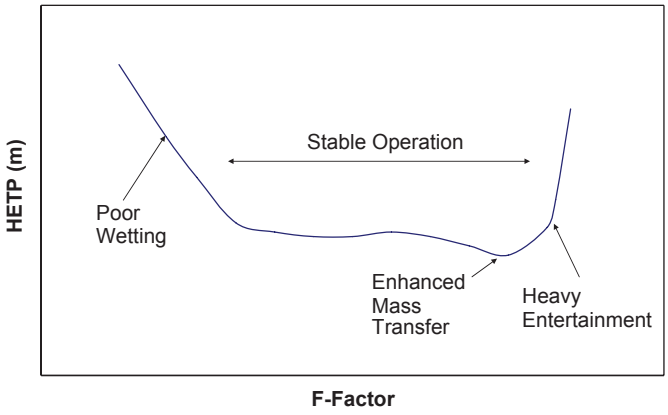

Fig. 17. General behaviour of packing efficiency.

$$\frac{k_G}{a_c D_G} = 5.23\, Re_G^{0.7} Sc_G^{1/3} (a_c d)^{-2} \tag{17}$$

$$H_L = \frac{u_L}{k_L a_e} \tag{18}$$

$$H_G = \frac{u_G}{k_G a_e} \tag{19}$$

$$HTU = H_G + \lambda H_L \tag{20}$$

$$HEPT = HTU \left(\frac{\ln \lambda}{\lambda - 1} \right) \tag{21}$$

The uncertainty in the HETP measurements was also determined, and appears as error bars in the graph. The determination of molar composition by refractive index was the main source of uncertainty in the HETP measurements. The uncertainty in molar composition was approximately 2% for all samples. An error of 2% in molar composition results in an uncertainty of almost 10% in the HETP determination.

The experimental points correspond well to the predictions of the model, especially for *F*-factors greater than 0.4. Both the experimental method and the results can therefore be considered valid.

4.2.2. Foam HETP

The results of HETP experiments performed under total reflux with an initial composition of 30 %molar cyclohexane/70 %molar *n*-heptane are presented in Fig. 16. The results of an additional test using a lower starting molar composition of cyclohexane (20 %molar) are also plotted to determine whether the starting composition influenced the performance.

As in the Raschig ring experiments, the HETP initially decreased with increasing gas and liquid velocities inside the packing until a constant value (0.2 m) was reached at ($0.5\,Pa^{0.5}$). HETP values for low *F*-factor are higher because of the bad wetting of packing. This is similar to the behaviour described for other packing materials (Kister, 1992; Bennet, 2000) (Fig. 17), with an initial decrease in HETP followed by an increase to the limiting value at the flooding point. In the present case, the decrease of HETP with *F*-factor was evident, but the HETP at the flooding point could not be obtained due to the instability of the column.

The HETP curves for both starting compositions were identical within the range of experimental uncertainty, indicating that the starting composition does not influence HETP.

As with the hydrodynamic data, HETP can be compared with other packings but caution must be exercised when comparing with the HETP results of other packings. In addition to differences in the dimensions of the test columns, there are variations in the overall

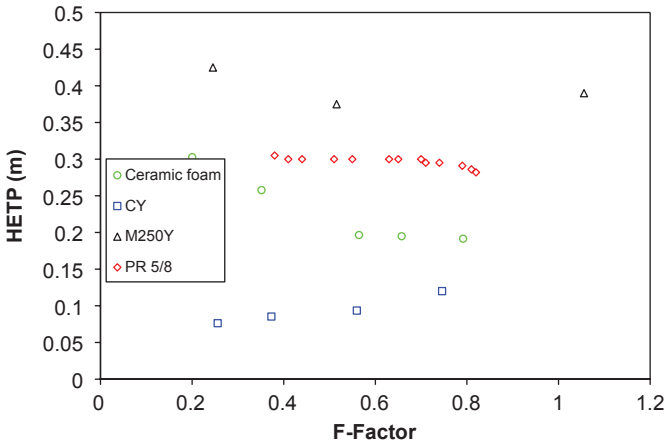

Fig. 18. Comparison of HETP for ceramic foam, M250Y, CY, and PR 5/8.

distillation system design and operating pressure. Fig. 18 contains a rough comparison of the following systems:

- Sulzer M250Y with cyclohexane/*n*-heptane mixture at 1.65 bar ($250\,m^2/m^3$ specific area) (Schultes and Chambers, 2007).
- Sulzer CY with chlorobenzene/ethylbenzene mixture at 0.4 bar ($700\,m^2/m^3$ specific area) (Kister, 1992).
- Pall rings (5/8 in) with methanol/2-propanol mixture at atmospheric pressure ($360\,m^2/m^3$ specific area) (Wen et al., 2003).

The experimental HETP values of ceramic foam fell between 0.2 and 0.3 m, corresponding to approximately 4–5 theoretical stages per metre. The mass transfer efficiency of the foam packing is higher than M250Y and P/R 5/8 but lower than CY, in accordance with the specific area for each packing. Therefore, the foam packing can be considered to have very good mass transfer performance.

The performance may also be compared by plotting number of theoretical stages per metre (NTSM) as a function of the pressure drop (Fig. 19). This represents a compromise between the hydrodynamic behaviour and the mass transfer efficiency of the packing. The ceramic foam exhibits intermediate performance, higher than M250Y and PR 5/8 in but lower than CY.

5. Conclusion

This paper presents a detailed investigation of the use of SiC ceramic foam as a distillation packing material. The principal

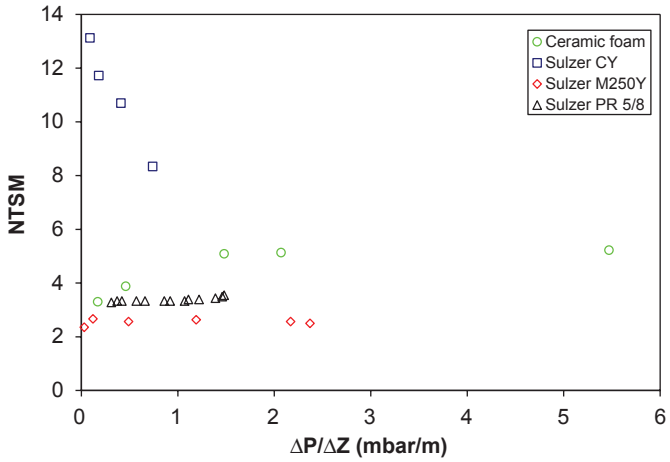

Fig. 19. Number of theoretical stage per metre (NTSM) in function of pressure drop for ceramic foam, M250Y, CY, and PR 5/8.

hydraulic characteristics of the foam were experimentally determined for gas–liquid countercurrent flow using an air–water system. The performance in terms of pressure drop per unit height and flooding behaviour was quite low compared with classical distillation packing materials (M250Y, CY, and Pall rings).

The liquid hold-up of the foam packing increased with increased liquid–gas loading in the loading zone, and the liquid hold-up was greater than other classical packing materials. The efficiency of the mass transfer was determined over the entire operating range using a cyclohexane/*n*-heptane system at atmospheric pressure under total reflux. The mass transfer performance was very good, with a HETP of 0.2 m and increasing mass transfer with increasing gas and liquid superficial velocities inside the packing.

Ergun's equation and the approach of Lacroix et al. (2007) were used to predict the pressure drop of the packing under dry and wet conditions. The agreement between predicted pressure drop and experimental results is quite well here although Incerra Garrido et al. (2008) have shown that Lacroix model is not very convenient for prediction of pressure drop and proposed a new empirical model. In this case, the Lacroix model is used because foam used in this work and foam sample studied by Lacroix et al. (2007) are provided by the same manufacturer. Nevertheless, this model is used by being aware of the fact that it is limited to our foam. The dynamic liquid hold-up was modelled as a function of the liquid phase Reynolds number.

Based on these results, ceramic foams could be considered as a good potential packing for distillation, however the applications would be limited by the low capacity.

The ceramic foam employed in this study exhibits other interesting properties:

- corrosion resistance,
- adaptability of the foam geometry to increase performance through structural modification, and
- the β-Sic material is well adapted to catalyst coating, introducing potential applications in reactive distillation

In the target application of reactive distillation, the low capacity does not represent a real disadvantage because the flowrates are lower. Moreover, increased liquid hold-up at low *F*-factors implies a high residence time, which would be favourable to the reaction. Tests of catalyst coatings on the foam and reaction kinetics measurements constitute the next step of the study.

Notation

a	window diameter of foam, m
a_c	specific surface area, m^2/m^3
a_e	effective interfacial area for gas–liquid contact, m^2/m^3
a_{GL}	interfacial liquid area per unit volume, m^2/m^3
aw	wetting surface area of the packing, m^2/m^3
A	pre-exponential parameter in wet pressure drop correlation
AC	compressed air
B	exponent in Reynolds number (Re) in wet pressure drop correlation
Cg	loading factor at flooding, $m\,s^{-1}$
d	packing nominal dimension, m
d_P	mean particle diameter, m
d_S	strut diameter, m
D_G, D_L	gas and liquid phase diffusion coefficient, $m\,s^{-2}$
D_p	pore diameter, m
E_1, E_2	constants in Ergun's equation
F	gas load, $Pa^{0.5}$
Fg	geometrical function, dimensionless
g	acceleration due to gravity, $9.81\,m\,s^{-2}$
G	gas mass flowrate, $kg\,s^{-1}\,m^{-2}$
Gf	mass flowrate at flooding point, $kg\,s^{-1}\,m^{-2}$
h_Ld	dynamic liquid hold-up
h_Ls	static liquid hold-up
h_Lt	total liquid hold-up
H_G	height of gas transfer unit, m
H_L	height of liquid transfer unit, m
HETP	height equivalent to a theoretical plate, m
HTU	height of a transfer unit, m
k_G	gas phase mass transfer coefficient, $m\,s^{-1}$
k_L	liquid phase mass transfer coefficient, $m\,s^{-1}$
k_1	viscous permeability parameter, m^2
k_2	inertial permeability parameter, m
K	permeability, m^2
L	mass liquid flowrate, $kg\,s^{-1}\,m^{-2}$
m	parameter in Fg
n	parameter in Fg
NTSM	number of theoretical stage per metre
P	pressure, mbar
PI	pressure indicator
PPI	pores per inch
$\Delta P/\Delta L$	pressure drop per unit packed height, $mbar\,m^{-1}$
Re_L, Re_G	liquid and gas phase Reynolds number
Sc_L, Sc_G	liquid and gas phase Schmidt number
u_0	superficial velocity, $m\,s^{-1}$
u_G	superficial gas velocity, $m\,s^{-1}$
u_L	superficial liquid velocity, $m\,s^{-1}$
X	Sherwood abscissa
Z	height, m

Greek letters

β	inertial coefficient, m^{-1}
ε	open void fraction, %
ε_h	hydrodynamic relevant porosity
λ	stripping factor
μ	fluid viscosity, $Pa\,s^{-1}$
μ_G, μ_L	dynamic viscosity of gas and liquid, $Pa\,s^{-1}$
ρ	fluid density, $kg\,m^{-3}$
ρ_G, ρ_L	density of gas and liquid, $kg\,m^{-3}$
ϕ	cell diameter, μm

Acknowledgements

The authors gratefully acknowledge Sicat Company for providing SiC foam samples and also for their support and discussions.

References

Bennet, D.L., 2000. Optimize distillation columns part II: packed column. Chem. Eng. Prog. 96 (5), 27–34.
Bhattacharya, A., Calmidi, V.V., Mahajan, R.L., 2002. Thermophysical properties of high porosity metal foams. Int. J. Heat Mass Transfer 45, 1017–1031.
Buchanan, J.E., 1969. Pressure gradient and liquid hold-up in irrigated packed towers. Ind. Eng. Chem. Fundam. 8, 502–511.
Chin, P., Sun, X., Roberts, G.W., Spivey, J.J., 2006. Preferential oxidation of carbon monoxide with iron-promoted platinum catalysts supported on metal foams. Appl. Catal. A: Gen. 302, 22–31.
Despois, J.F., Mortensen, A., 2005. Permeability of open-pore microcellular materials. Acta Mater. 53, 1381–1388.
Dmitrieva, G.B., Berengarten, M.G., Klyushenkova, M.I., Pushnov, A.S., 2005. Calculation of hydrodynamic parameters for regular structured packings. Chem. Pet. Eng. 41, 625–633.
Dukhan, N., 2006. Correlation for the pressure drop for flow through metal foam. Exp Fluids 41, 665–672.
Ellenberger, J., Krishna, R., 1999. Counter current operation of structured catalytically packed distillation columns: pressure drop, holdup and mixing. Chem. Eng. Sci. 54, 1339–1345.
Giani, L., Groppi, G., Tronconi, E., 2005. Mass-transfer characterization of metallic foams as supports for structured catalysts. Ind. Eng. Chem. Res. 44, 4993–5002.
Incerra Garrido, G., Patcas, F.C., Lang, S., Kraushaar-Czarnetzki, B., 2008. Mass transfer and pressure drop in ceramic foams: a description for different pore sizes and porosities. Chem. Eng. Sci. 63, 5202–5217.
Kister, H., 1992. Distillation Design. McGraw-Hill, New York.
Kolodziej, A., Jaroszynski, M., Bylica, I., 2004. Mass transfer and hydraulics for KATAPAK-S. Chem. Eng. Process. 43, 457–464.
Lacroix, M., Nguyen, P., Schweich, D., Huu, C.P., Poncet, S.S., Edouard, D., 2007. Pressure drop measurements and modeling on SiC foams. Chem. Eng. Sci. 62, 3259–3267.
Leong, K.C., Jin, L.W., 2006. Characteristics of oscillating flow through a channel filled with open cell metal foam. Int. J. Heat Fluid Flow 27, 144–153.
Muzen, A., Cassanello, M.C., 2005. Liquid holdup in columns packed with structured packings: countercurrent vs. cocurrent operation. Chem. Eng. Sci. 60, 6226–6234.
Olujic, Z., Seibert, A.F., Fair, J.R., 2000. Influence of corrugation geometry on the performance of structured packings: an experimental study. Chem. Eng. Process. 39, 335–342.
Onda, K., Takeuchi, H., Okumoto, Y., 1968. Mass transfer coefficients between gas and liquid phases in packed columns. J. Chem. Eng. Jpn. 1, 56–62.
Pestryakov, A.N., Yurchenko, E.N., Feofilov, A.E., 1996. Foam-metal catalysts for purification of waste gases and neutralization of automotive emissions. Catal. Today 29, 67–70.
Pestryakov, A.N., Lunin, V.V., Petranovskii, V.P., 2007. Catalysts based on foam materials for neutralization of waste gases. Catal. Commun. 8, 2253–2256.
Richardson, J.T., Peng, Y., Remue, D., 2000. Properties of ceramic foam catalyst supports: pressure drop. Appl. Catal. A: Gen. 204, 19–32.
Richardson, J.T., Garrait, M., Hung, J.K., 2003. Carbon dioxide reforming with Rh and Pt–Re catalysts dispersed on ceramic foam supports. Appl. Catal. A: Gen. 255, 69–82.
Schultes, M., Chambers, S., 2007. How to surpass conventional and high capacity structured packings with raschig super-pak. Chem. Eng. Res. Des. 85 (A1), 118–129.
Sirijaruphan, A., Goodwin Jr., J.G., Rice, R.W., Wei, D., Butcher, K.R., Roberts, G.W., Spivey, J.J., 2005. Metal foam supported Pt catalysts for the selective oxidation of CO in hydrogen. Appl. Catal. A: Gen. 281, 1–9.
Stemmet, C.P., Jongmans, J.N., Van der Schaaf, J., Kuster, B.F.M., Schouten, J.C., 2005. Hydrodynamics of gas–liquid counter-current flow in solid foam packings. Chem. Eng. Sci. 60, 6422–6429.
Stemmet, C.P., Meeuwse, M., Van der Schaaf, J., Kuster, B.F.M., Schouten, J.C., 2007. Gas–liquid mass transfer and axial dispersion in solid foam packings. Chem. Eng. Sci. 62, 5444–5450.
Subawalla, H., Castor Gonzalez, J., Seibert, A.F., Fair, J.R., 1997. Capacity and efficiency of reactive distillation bale packing: modeling and experimental validation. Ind. Eng. Chem. Res. 36, 3821–3832.
Topin, F., Bonnet, J.P., Madani, B., Tadrist, L., 2006. Experimental analysis of multiphase flow in metallic foam: flow laws, heat transfer and convective boiling. Adv. Eng. Mater. 8 (9), 890–899.
Wen, X., Afacan, A., Nandakumar, K., Chuang, K.T., 2003. Geometry-based model for predicting mass transfer in packed columns. Ind. Eng. Chem. Res. 42, 5373–5382.
Winé, G., Tessonnier, J.P., Rigolet, S., Marichal, C., Ledoux, M.J., Pham Huu, C., 2006. Beta zeolite supported on a [beta]-SiC foam monolith: a diffusionless catalyst for fixed-bed Friedel–Crafts reactions. J. Mol. Catal. A: Chem. 248, 113–120.